Raman Microspectroscopic Mapping: A Tool for the Characterisation of Polymer Surfaces

*Imelda Keen, Llewellyn Rintoul, Peter M. Fredericks**

Centre for Instrumental & Developmental Chemistry, Queensland University of Technology, PO Box 2434, Brisbane, Qld 4001, Australia

Summary: Raman mapping by point illumination of polymer surfaces is discussed with examples taken from the plasma treatment of polypropylene (PP) and subsequent grafting of polystyrene (PS). Maps can be constructed for surface properties such as crystallinity, blend components and distribution of grafted PS. The Raman sampling volume was estimated for confocal operation using a 50x objective lens.

Introduction

Many polymer surfaces show a heterogeneity of molecular structure because of variability of properties such as crystallinity, orientation, distribution of components in blends, distribution of additives or fillers, preferential oxidation or degradation, or distribution of grafted copolymer. Raman microspectroscopy is an ideal tool to investigate such surfaces because it has advantages in terms of spatial resolution and the simplicity of the measurement. In particular, Raman has significant advantages over infrared (IR) microspectroscopy. IR microspectroscopy has a spatial resolution which is typically governed by the diffraction limit and therefore the best achievable with a laboratory spectrometer is in the range 10-15 μm.[1,2] Furthermore, at this spatial resolution signal-to-noise ratio is often a problem. By contrast, it is simple to achieve a beam waist of better than 1 μm in Raman microspectroscopy by the use of a visible laser source and a 50x objective lens.[3]

The nature of the polymer surface has considerable effect on the spectrum in IR microspectroscopy. A smooth surface will produce a specular reflectance spectrum which may be treated with the Kramers-Krønig transformation to calculate the absorption index spectrum.[4] A matt surface will produce a diffuse reflectance spectrum which can be converted to Kubelka-Munk units to improve linearity. However, many real polymer surfaces produce a mixed IR spectrum which is usually difficult to interpret. An alternative is to use an attenuated total reflectance (ATR) objective lens which generally produces a readily interpretable spectrum from any polymer surface.[5] The disadvantages of the ATR objective are worse spatial resolution and the possibility of surface damage because direct contact with

 CCC 1022-1360/00/$ 17.50+.50/0

the sample is necessary.

By contrast, Raman microspectroscopy does not depend on the nature of the surface because the incident light is focussed to less than 1 μm. Occasionally, sample fluorescence is a problem and swamps the Raman signal. Often this can be overcome by using longer wavelength excitation, although this will lead to a larger spatial resolution.

Raman mapping or imaging is the process of studying a larger area of the surface.[6,7] Imaging refers to the experiment which utilises global illumination of the area under study which is then imaged directly onto a CCD detector. In the past, imaging has only been possible at a single Raman wavelength, or a narrow band of wavelengths.[8] However, recently instrumentation has become available which allows the complete Raman spectrum to be collected for each pixel. Raman mapping is an equivalent procedure which uses point illumination to obtain the spectrum at a single point on the sample.[9,10] The sample is then moved under computer control so that spectra are gathered in a grid pattern over an area of the sample. The spectra are saved as a multifile and may be displayed and interpreted using commercially available software. Raman mapping requires the collection of large numbers of spectra and therefore may be very time-consuming. However, a large region of the Raman spectrum may be collected at each point, providing a large amount of data for further interpretation. Raman images may also be collected by a line scanning process.[11]

This paper discusses a number issues concerned with the practical and theoretical application of Raman mapping to polymer surfaces. Illustrative examples are drawn from work in our laboratory on plasma treated and grafted polymer surfaces.

Experimental

Raman spectra were collected on a Renishaw System 1000 Raman microprobe spectrometer (Renishaw plc. Wotton-under-Edge, UK) equipped with a He-Ne laser emitting at 632.8 nm. An Olympus MD Plan microscope with a 50x objective lens (numerical aperture 0.75) was used to focus the laser to a spot size of around 1 μm. The laser power was about 8 mW at the sample. Confocal operation was achieved by setting the slit width to 15 μm and by masking the CCD detector to an image height of 4 pixels.

Samples were small pieces of polymer around 5 mm x 5 mm in size. Typically, these pieces were embedded in a resin (Araldite^{TM}) which was cured overnight at 60°C. The sample/resin was then cut with a sharp scalpel to expose a fresh polymer face which was then polished with increasingly finer grades of emery paper. The sample was then mounted firmly on the

microscope stage prior to Raman mapping.

Results and Discussion

From where in the sample is the spectrum measured?

There are two aspects to be considered to answer the question: from where on the sample is the spectrum measured? Namely, where does the laser beam impinge onto the sample and from where is the scattered light collected by the microscope/spectrometer. The beam of a HeNe laser has a spherical wavefront and a Gaussian radial amplitude distribution. The beam radius is defined by the 1/e point on the Gaussian distribution curve. It is important to remember that by definition 14% of the total power lies outside the nominal beam radius. When focussed with a lens, a collimated Gaussian beam does not converge to a point but rather to a beam waist (Figure 1) and retains its Gaussian distribution. As a beam propagates beyond the beam waist it at first remains almost constant in diameter forming a collimated region or "focal tube" before diverging linearly in the far field. The radius of the waist, r_0, is given by $f\lambda/\pi r$ and the length of the focal tube is given by $2\pi r_0^2/\lambda$, where f is the focal length, λ is the laser wavelength and r is the initial collimated beam radius.[12]

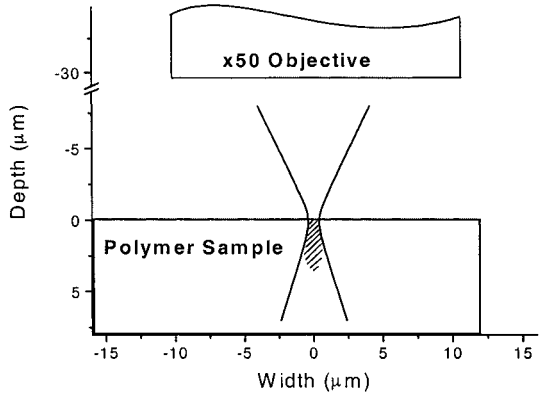

Figure 1. Diagram showing the estimated location of excitation light, and that part of the sample (shaded) from which the signal originates.

From a design point of view, where the object is to obtain the smallest possible laser spot to maximise the potential spatial resolution, the equations suggest that a large collimated input

beam is desirable. However once the laser beam is expanded to the point where it begins to be truncated by the aperture of the lens there is an associated power loss and additional diffraction consequences. In any case the smallest spot that can be achieved is limited by diffraction to little more than the laser wavelength in diameter with a collimated region around 6 wavelengths long.

In a confocal microscope light collected from the focal plane is imaged onto a confocal aperture before reaching the eyepiece (or detector). The size of the confocal aperture in conjunction with the magnification of the optical system determines the diameter of the spot from where light is collected on the sample. Light from deeper within the sample (out of focus regions) forms a blurry, larger image on the confocal aperture and only on- or near-axis rays will be transmitted. Thus, the further from the focal plane the smaller the portion of light collected. The smallest region within the sample that may be isolated by a confocal microscope depends on the physical size of the confocal aperture and is limited, like the case of the laser illumination, by diffraction considerations to slightly more than a wavelength in diameter and a few wavelengths in depth. The depth discrimination of a confocal Raman microscope confers the ability to "optically section" the sample. This has been comprehensively discussed in recent publications by several workers.[13-15] Optical sectioning of the sample is beyond the scope of this article but some of the considerations apply even when the microscope is focussed on the surface because part of the Raman signal is generated beneath the surface of the sample. It is important to acknowledge the relative contribution that the signal from deeper within the sample makes to the measurement.

Under laser illumination, the Raman signal generated by the diverging beam beyond the confocal region contributes little to the measured signal because it will be rejected if the confocal aperture is set small enough. Maximum spatial resolution in all 3 dimensions of the sample is achieved with fast short focal length lenses and with the microscope set for maximum confocality. As the confocal parameter is relaxed by increasing the size of the confocal aperture, the lateral spatial resolution at the focal plane remains the same as the laser spot size but Raman signal from a deeper and broader section of the sample makes an increased contribution to the total signal, blurring the spatial information of the measurements.

In the Renishaw Raman microscope the confocal aperture is formed by the slit of the spectrograph along one axis and a selectable number of detector pixels on the orthogonal axis. Despite the lack of a conventional confocal aperture the same considerations apply. In the experiments described in this paper, confocal operation was achieved by setting the slit width

to 15 μm and by masking the CCD detector to an image height of 4 pixels. With these settings and using a 50x dry microscope objective of 0.75 numerical aperture, the sample volume is shaped somewhat like an ellipsoid with the top end truncated at the surface of the sample and is roughly 1 micron in diameter and 3-4 microns long.

Experimental Difficulties

The above discussion applies if the surface is flat and horizontal so that all parts to be mapped are in focus. In order to achieve this situation, it is necessary to spend some time placing the sample on the stage. The focus at all points should be checked and the sample adjusted if necessary. If the sample is not at the focus of the incident light beam, then two things happen, (i) the spot size becomes larger which changes the spatial resolution, and (ii) the incident power per unit area is diminished resulting in a less intense spectrum and a reduced signal-to-noise ratio. Since spectra are normalised before analysis the latter point may not be significant depending on the severity of the signal-to-noise deterioration. Many polymer surfaces, such as those which have been heterogeneously grafted, cannot be flat to within 1 μm which would be required for optimum focus. In this case it should be realised that the spatial resolution is merely nominal.

Commercial Raman microprobe spectrometers are now available which incorporate an autofocus feature. This obviates the problems mentioned above, but may add up to 10 s per spectrum which will become significant if hundreds of spectra are to be collected.

The time taken for point by point measurements can be excessive if large areas are to be studied at high spatial resolution. Our measurements on a 50 μm x 50 μm area at a spatial resolution of 1 μm required the collection of 2601 individual spectra. The total measurement time was around 16 h. Obviously one only studies a surface with a spot size of 1 μm with a step size of 1 μm where the heterogeneity of the surface warrants it. In other words, where the surface features are approximately micron sized. For larger features, a larger spot size, achieved by using an objective lens of lower magnification, together with a larger step size will be adequate to characterise the surface.

Measurement of Surface Properties

Crystallinity

Semi-crystalline polymers are common and it is of interest to determine the crystallinity at points on the surface as this may affect further surface reactions. Vibrational spectroscopy provides a means to estimate crystallinity. IR spectroscopy has been the main tool, but Raman

spectroscopy is also useful.[10] For example, for polypropylene (PP) a measure of crystallinity may be calculated from the area ratio of bands at 998 and 973 cm^{-1} which correspond to C-C stretching bands of ordered and amorphous PP, respectively.[16] Figure 2 shows a Raman crystallinity map based on these bands for a PP surface measuring 50 μm x 50 μm, mapped at 1 μm intervals. Clearly, the crystallinity varies across the surface, but is relatively low overall as the area ratio varies between only about 0.1 and 0.5. On other more crystalline samples we have measured this ratio as high as 1.1.

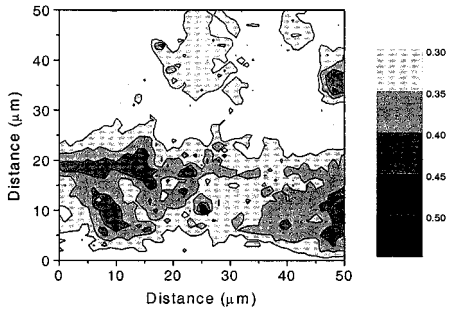

Figure 2. Map of the area ratio of the Raman bands at 998 and 973 cm^{-1} for a PP substrate, which is a measure of the crystallinity of the surface.

We have not attempted to quantify crystallinity from the Raman measurements. This would be difficult because although it is relatively simple to measure % crystallinity of PP on a macro sample, for example by differential scanning calorimetry, it is not possible to know the exact crystallinity within the small sampling volume of a Raman microprobe.

The measurement of crystallinity, i.e. the proportion of the sample that exists within crystallites, is complicated by the variation in orientation of those crystallites. Certain polymer processing methods, such as fibre drawing, significantly change the orientation of the sample so that a high level of anisotropy may be achieved. At the same time the crystallinity of the sample may also increase significantly. Quite often literature methods for crystallinity determination using vibrational spectroscopy ignore orientation effects. However, for Raman spectroscopy this is likely to lead to errors because the laser source is almost always polarised so that the spectrum is affected by both the crystallinity and the orientation of the sample. As noted above, we have used the area ratio of bands at 998 and 973 cm^{-1} as a measure of crystallinity in PP, although they are in fact related to the formation of regular helices in the PP chains[16]. Large changes in sample orientation may lead to an error in this measurement.

Arruebarrena de Báez et al[17] have proposed the use of the bands at 842 and 809 cm^{-1} for the estimation of PP orientation, but they also concede that variation in crystallinity may affect the measurement. It therefore remains difficult to separate the two effects of crystallinity and orientation when making Raman measurements. One possible approach might be to measure crystallinity with a depolarised laser beam by inserting a quartz wedge polarisation scrambler. This should give a more reliable estimation of crystallinity independent of variation in orientation. However, the insertion loss caused by the polarisation scrambler device may have an impact on the signal-to-noise ratio of the spectra.

Distribution of Components

One of the most important uses of Raman mapping is to measure the distribution of the different components of a polymer.[9,10] This could include, for example, blend components, additives, and fillers. In our work we have studied materials used in combinatorial chemistry which are composed of PP containing about 15 mole % ethylene propylene rubber (EPR) as a toughening agent. Distinct Raman bands can be found for the EPR which comprises mainly ethylene units and can be distinguished from the propylene groups of the PP. The most useful bands were found to be the 1064 cm^{-1} band of the EPR and the 1220 cm^{-1} band of the PP. If the scattering cross-section for these bands is known from standard materials, then a semiquantitative calculation of EPR concentration is possible.[10]

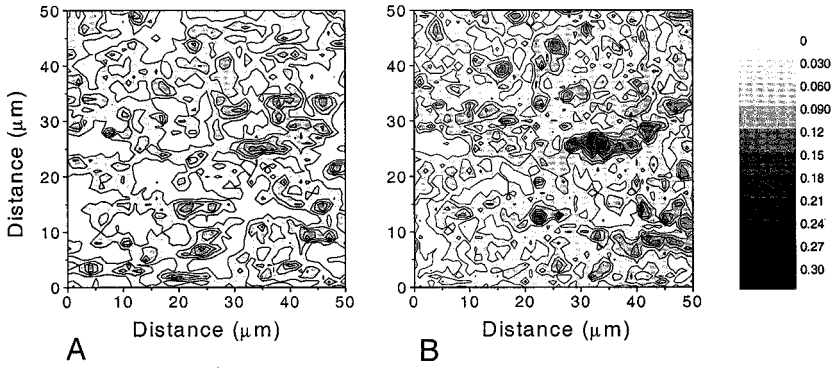

Figure 3. Raman maps of the distribution of EPR on a PP surface (A) before plasma treatment and (B) after plasma treatment.

Figure 3 shows Raman maps of the EPR distribution for a 50 μm x 50 μm section of the polymer surface, before and after plasma treatment. The scale of the maps is calculated mole % EPR, rather than band ratio which was used for the crystallinity map. From the maps it is clear that the surface EPR increases slightly after plasma treatment because of the greater susceptibility of PP to etching or ablation in the plasma.

Another example from our work is the graft polymerisation of the PP/EPR substrates with polystyrene (PS). We found the grafting of PS to be heterogeneous across the surface. PS is easily detected on the PP surface by the aromatic C=C stretching band at 1601 cm^{-1}, but because of spectral overlap it is difficult to find a band to provide a clear measure of the PP. It proved necessary to decompose the CH_2 deformation band at 1450 cm^{-1} into PS and PP contributions. The resulting Raman map (Figure 4A) shows the distribution of PS on a 50 μm x 50 μm PP/EPR surface after graft polymerisation. The heterogeneity of the grafting is clear. Comparison of this map with maps of exactly the same area of surface before and after plasma treatment showed that the EPR part of the PP/EPR blend was being preferentially grafted with PS and that surface crystallinity was less significant in determining the graft concentration.[10] The Raman map was validated by comparison with the scanning electron microscope (SEM) image of approximately the same part of the sample (Figure 4B). In the SEM image the regions of high PS are seen as white areas and a good match can be seen between the Raman and SEM images.

Polar Functionality

It is significant for our work to be able to quantify the various oxygen functional groups created on the surface by plasma treatment. Unfortunately, Raman spectroscopy is relatively insensitive to polar functional groups and it is difficult to detect the low level of functionality particularly when it is restricted to the surface. Infrared microspectroscopy is more sensitive and better suited to this task, but as mentioned before, the spatial resolution is typically much worse than for Raman microspectroscopy. In situations where the level of functional groups is high, weak bands may be seen in the Raman spectra, but long measurement times may be needed to achieve a useful signal-to-noise ratio. Blakey and George[18] were able to map the degree of oxidation of photo-oxidised PP despite a relatively poor signal-to-noise ratio.

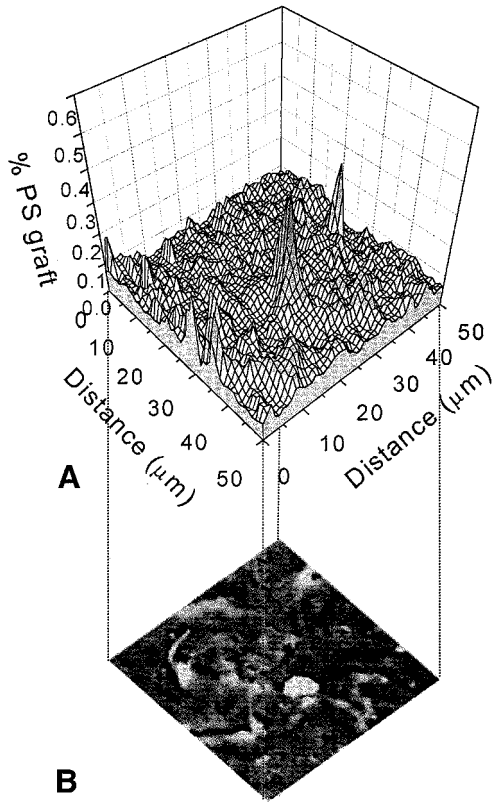

Figure 4. Comparison of (A) Raman map of the grafted PS distribution on a predominantly PP surface with (B) an SEM micrograph of approximately the same area of the surface.

1-Dimensional Mapping

There are many instances when 2-D mapping as described above is unnecessary and sufficient information can be obtained more quickly by collecting spectra along a line through the area of interest. In our work we have studied the graft polymerisation of PS onto PP using γ-irradiation. In this case a relatively thick layer of PS is grafted to the PP surface which then becomes quite homogeneous. The required information is the thickness of the PS layer and the thickness of the interphase layer between the PS layer and the PP substrate. This information is obtained by sectioning the sample perpendicular to the surface and collecting spectra at intervals from the surface through the graft layer and into the substrate.

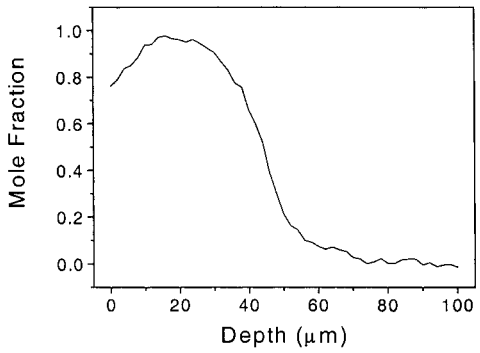

Figure 5. PS distribution in a cross-section of PP substrate after grafting reactions with styrene.

Figure 5 shows a typical example where the calculated mole fraction of PS is plotted against distance from the surface for spectra collected at 2 μm intervals. It can be seen that in this case the PS layer is about 40 μm thick, while the interphase layer of mixed PS/PP is about 30 μm thick. One interesting feature is that the grafted layer is never 100% PS. In the spectrum of every point in the grafted layer there is always evidence of a small amount of PP, and close to the surface the amount of PP seems to increase somewhat. This is evidence that grafting is not the simplistic process often depicted of the grafted layer growing away from the surface, but rather the graft seems to grow into the substrate and intermix with the PP as it expands.

We have also used 1-dimensional Raman mapping to study PP substrates which have been plasma treated before being grafted with PS. The substrate was sectioned and the distribution of PS measured by Raman microspectroscopy. It was found that the conditions of plasma treatment had a profound effect on the PS distribution. Figure 6 shows results for 400 μm sections of a PP/EPR substrate. Diagram A shows that when an argon plasma, followed by exposure to oxygen, is used, the PS is distributed heterogeneously throughout the whole substrate with little difference between the concentration at the surface and that found in the interior of the substrate. However, if an oxygen plasma is used, then the grafting is more homogeneous (i.e. the graph in Diagram B is smoother) and more graft is seen near the surfaces than in the interior of the substrate. We believe that this difference is related to the fact that an argon plasma generates considerable vacuum UV radiation which penetrates the substrate, whereas an oxygen plasma tends to generate oxygen radicals, which are much less penetrating.

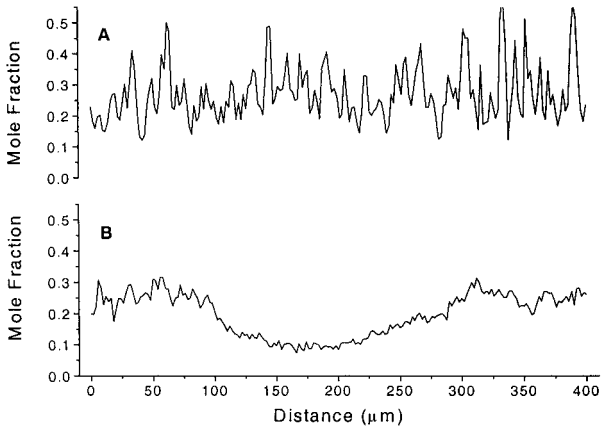

Figure 6. PS Distributions determined by 1-dimensional mapping for cross-sections of PP/EPR substrates which have been plasma treated with (A) argon plasma, followed by exposure to oxygen; and (B) oxygen plasma.

An alternative approach of confocal Raman microspectroscopy has been used by Mattsson et al[19] to investigate PS grafting into poly(vinylidene fluoride) membranes. Using the technique of "optical slicing" or "z-scanning" they were able to measure PS concentrations in the interior of the membrane without any sample preparation such as sectioning and polishing. However, Everall has recently cast serious doubts on this approach because of distortion of the beam as it passes into the sample.[13,14]. The use of an immersion lens improves matters, but it is recommended that, where possible, a physical cross-section be obtained and the exposed surface mapped in the usual way.

Conclusion

Raman mapping has been shown to be a useful tool for the characterisation of polymer surfaces. Such surface properties as the variation in crystallinity, and distribution of components in a blend may be measured and mapped. While it is difficult to quantify crystallinity, component proportions may be calculated in a semiquantitative manner if Raman cross-sections are known from standard materials. Under confocal conditions the signal in our spectrometer is estimated to come from an ellipsoid with the top end truncated at the surface of the sample and with dimensions approximately 1 μm in diameter and 3-4 μm long.

Acknowledgment

We thank Firas Rasoul and Joe Maeji of Polymerat Pty Ltd for supplying the samples and for helpful discussions.

[1] J. E. Katon, *Vib. Spectrosc.*, **1994**, *7*, 201.
[2] J. A. Reffner, P. A. Martoglio, "Uniting Microscopy and Spectroscopy" in *Practical Guide to Infrared Spectroscopy* (H. J. Humecki, ed.), Marcel Dekker, New York, 1995, p. 41.
[3] A. J. Sommer, "Raman Microscopy" in *Modern Techniques in Applied Molecular Spectroscopy* (F. M. Mirabella, ed.), John Wiley & Sons, New York, 1998, p. 291.
[4] J. M. Chalmers, N. J. Everall, S. Ellison, *Micron*, **1996**, *27*, 315.
[5] T. Buffeteau, B. Desbat, D. Eyquem, *Vib. Spectrosc.*, **1996**, *11*, 29.
[6] J. Barbillat, "Raman Imaging" in *Raman Microscopy: Developments and Applications* (G. Turrell and J. Corset, eds.), Academic Press, London, 1996, p. 379.
[7] A. Garton, D. N. Batchelder, C. Cheng, *Appl. Spectrosc.*, **1993**, *47*, 922.
[8] K. P. J. Williams, G. D. Pitt, B. J. E. Smith, A. Whitley, D. N. Batchelder, I. P. Hayward, *J. Raman Spectrosc.*, **1993**, *25*, 131.
[9] R. Appel, T. W. Zerda, W. H. Waddell, *Appl. Spectrosc.*, **2000**, *54*, 1559.
[10] I. Keen, L. Rintoul, P. M. Fredericks, *Appl. Spectrosc.*, **2001**, *55*, 984.
[11] J. Barbillat, P. Dhamelincourt, M. Delhaye, E. Da Silva, *J. Raman Spectrosc.* **1994**, *25*, 3.
[12] A.E. Siegman, *Lasers,* University Science Books, Mill Valley, CA, 1986, p675.
[13] N. J. Everall, *Appl. Spectrosc.*, **2000**, *54*, 773.
[14] N. J. Everall, *Appl. Spectrosc.*, **2000**, *54*, 1515.
[15] K. J. Baldwin and D.N. Batchelder, *Appl. Spectrosc.*, **2001**, *55*, 517
[16] T. Sundell, H. Fagerholm, H. Crozier, *Polymer*, **1997**, *37*, 3227.
[17] M. Arruebarrena de Báez, P. J. Hendra, M. Judkins, *Spectrochim. Acta*, **1995**, *51A*, 2117.
[18] I. Blakey, G. A. George, *Polym. Deg. Stab.*, **2000**, *70*, 269.
[19] B. Mattsson, H. Ericson, L. M. Torell, F. Sundholm, *J. Polym. Sci. Part A*, **1999**, *37*, 3317.